7 DOUGLAS, J.: 'Alternating direction methods for three space variables', *Numer. Math.*, 1962, **4**, pp. 41–63
8 YAMAUCHI, J., NIBE, M., and NAKANO, H.: 'Scalar FD-TD method for circularly symmetric waveguides', *Opt. Quantum Electron.*, 1997, **29**, pp. 451–460

Universal relations for coupling of optical power between microresonators and dielectric waveguides

A. Yariv

The most basic and generic configuration, which consists of a unidirectional coupling between a ring resonator and a waveguide, is considered. The fundamental working equations required to describe the associated power transfer are derived and the application of this geometry to a variety of optical phenomena is discussed. These phenomena include 'add/dropping' of optical beams, add/drop filtering and optical power switching.

The manipulation of coupling between optical waveguides and micro-resonators is shaping up as an important area of research and development [1, 2]. To analyse the exchange of optical power between a waveguide and a resonator we consider the basic geometry of Fig. 1. It consists of lossless coupling between an optical waveguide and a ring resonator. The nature of the coupling is not important for the purpose of our generic analysis. Under the conditions that a single unidirectional mode of the resonator is excited and that the coupling is lossless, we can describe the interaction by the matrix relation

$$\begin{vmatrix} b_1 \\ b_2 \end{vmatrix} = \begin{vmatrix} t & \kappa \\ -\kappa^* & t^* \end{vmatrix} \begin{vmatrix} a_1 \\ a_2 \end{vmatrix} \quad (1)$$

where the complex mode amplitudes b_i, a_i are normalised such that their squared magnitude corresponds to the modal power. The coupling matrix is unitary so that

$$|\kappa^2| + |t^2| = 1 \quad (2)$$

The specific form of κ is not needed for the purpose of this Letter. It depends on the particular coupling mechanism employed. A number of different schemes will be explored in a future publication. In the following, we will choose that input wave $a_1 = 1$ so that all the field amplitudes will be normalised to a_1. The transmission around the ring is given by

$$a_2 = \alpha e^{i\theta} b_2 \quad (3)$$

where α, the inner circulation factor, is real. For zero internal loss $\alpha = 1$. From eqns. 1 and 3 we obtain

$$b_1 = \frac{-\alpha + te^{-i\theta}}{-\alpha t^* + e^{-i\theta}} \qquad a_2 = \frac{-\alpha\kappa^*}{-\alpha t^* + e^{-i\theta}} \quad (4)$$

The transmission past the resonator in the input waveguide is

$$|b_1|^2 = \frac{\alpha^2 + |t|^2 - 2\alpha|t|\cos(\theta + \phi_t)}{1 + \alpha^2|t|^2 - 2\alpha|t|\cos(\theta + \phi_t)} \quad (5)$$

where $t = |t|\exp(i\varphi_t)$, while the total circulating power is

$$|a_2|^2 = \frac{\alpha^2(1 - |t|^2)}{1 - 2\alpha|t|\cos(\theta + \phi_t) + \alpha^2|t|^2} \quad (6)$$

Most of the interesting features of this resonator occur near resonance where $(\theta + \varphi_t) = m2\pi$, where m is some integer. At resonance

$$|b_1|^2 = \frac{(\alpha - |t|)^2}{(1 - \alpha|t|)^2} \qquad |a_2|^2 = \frac{\alpha^2(1 - |t|)^2}{(1 - \alpha|t|)^2} \quad (7)$$

The first part of eqn. 7 is of special interest. It shows that when $\alpha = |t|$, i.e. when the internal losses (represented by α) are equal to the coupling losses represented by ($|t|$), the transmitted power vanishes, i.e. $|b_1|^2 = 0$. This condition, known in the microwave field as that of *critical coupling* [3, 4] is due to perfect destructive interference in the outgoing waveguide between the transmitted field ta_1 and the internal field coupled into the output waveguide κa_2.

We note that all our central results depend only on t and α and are *independent of* the details of the coupling and *those of the resonator*. Their simplicity and form are reminiscent of the basic relations describing the Fabry-Perot etalon.

Fig. 2 shows, in *a*, the transmission and, in *b*, the internal circulating power against α for a given value of t. The dependence of the transmission on α near the critical coupling $\alpha = 1$ is particularly dramatic. Note that the internal power at $\alpha = |t|$ is a quarter of its value in the case of no internal loss, $\alpha = t$. The important implications for the control of the power flow by operating near the critical coupling point are obvious.

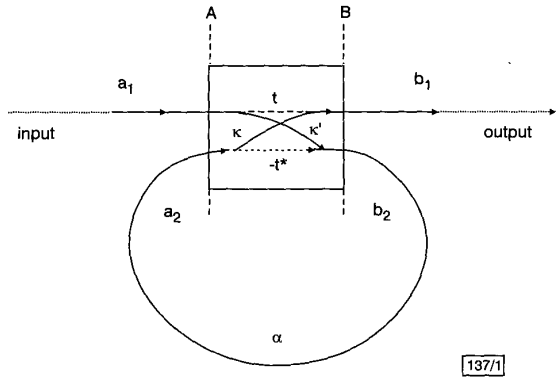

Fig. 1 *Generic description of dielectric waveguide coupled to ring resonator*

'Box' between planes A and B is not specified except for universal coupling parameters κ and t

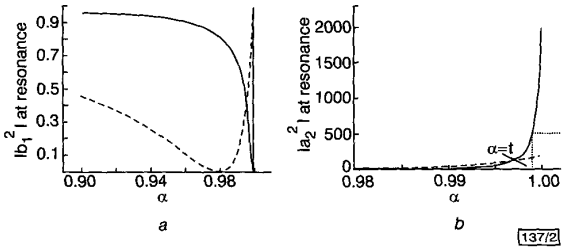

Fig. 2 *Straight waveguide power transmission and internal circulating power*

a Straight waveguide power transmission factor $|b_1|^2$ against internal loss α and coupling parameter t
——— $t = 0.999$
– – – – $t = 0.980$
b Internal circulating power $|a_2|^2$ against α with $|t|$ as parameter
——— $t = 0.999$
– – – – $t = 0.990$
Incident power $|a_1|^2 = 1$ W

Fig. 3 shows the transmission characteristics against frequency near critical coupling. We include the case of gain in the resonator so that $\alpha > 1$, but $\alpha|t| < 1$. In this case the transmission dip 'flips over' and the transmitted signal is amplified. The resonance peak in this case can be made arbitrarily narrow. When $\alpha|t| = 1$, we obtain according to eqn. 7 infinite transmission, i.e. *laser oscillation*. From eqn. 6 and $\theta = \omega L/c$, we obtain the full frequency width at half maximum (FWHM) in the high finesse case as

$$\Delta\omega_{FWHM} \cong \frac{2(1 - |t|^2)c}{L} = \frac{2\kappa^2 c}{L} \qquad \alpha = |t| \approx 1 \quad (8)$$

where L is the circumference of the ring and c the phase velocity of the ring mode. The finesse of the resonator is the ratio of the free spectral range $2\pi c/L$ to $(\Delta\omega)_{FWHM}$:

$$F = \frac{\pi}{(1 - |t|^2)} = \frac{\pi}{|\kappa|^2} \qquad \alpha = |t| \approx 1 \quad (9)$$

corresponding to a resonator figure of merit

$$Q = \frac{\omega}{(\Delta\omega)_{FWHM}} = \frac{\pi f L n_{eff}}{c_o(1 - |t|^2)} = \frac{\pi L n_{eff}}{\lambda_0|\kappa|^2} \quad (10)$$

where $c = c_o/n_{eff}$.

Another geometry of practical interest is illustrated in Fig. 4 where the resonator is also coupled to a second waveguide. From the point of view of the original waveguide the presence of the second (lower) waveguide merely modifies the internal loss parameter from α to $\alpha|t_2|$ (the '1' and '2' subscripts now refer to the 'original' and 'new' waveguides, respectively). All the expressions, and the curves, given above apply, provided we put $t \rightarrow t_1$ ($\kappa \rightarrow \kappa_1$) and $\alpha \rightarrow \alpha|t_2|$. The output power $|a_r|^2$ from the second guide is of special interest. At resonance

$$|a_r|^2 = \frac{(1-|t_1|^2)(1-|t_2|^2)\alpha}{(1-\alpha|t_1 t_2|)^2} \qquad (11)$$

Full transfer of power from the input guide to the output guide, i.e. $|a_r|^2 = 1$, occurs when the two following conditions are satisfied: $\alpha = 1$ (negligible internal losses) and $|t_1| = |t_2|$ (identical coupling) The transfer of power between waveguides can thus be controlled by small changes in $|t_1|$ or $|t_2|$.

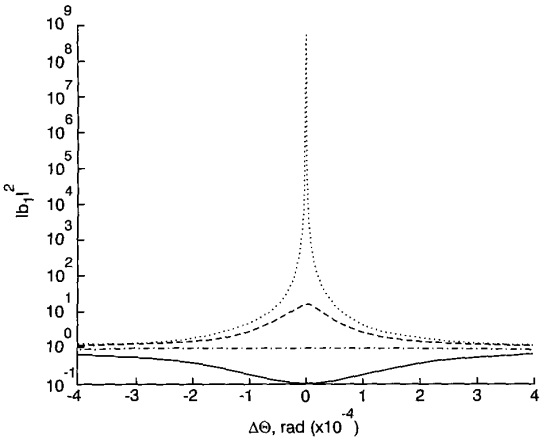

Fig. 3 *Waveguide power transmission against frequency* ($\theta = \omega L/c$) *with internal loss factor* α *as a parameter*

$|t| = 0.9998$

$\alpha < 1$ corresponds to passive loss resonator, $\alpha > 1$ corresponds to internal gain

——— $\alpha = 0.9998$

–·–·– $\alpha = 1.0000$

– – – – $\alpha = 1.00006$

····· $\alpha = 1.0001$

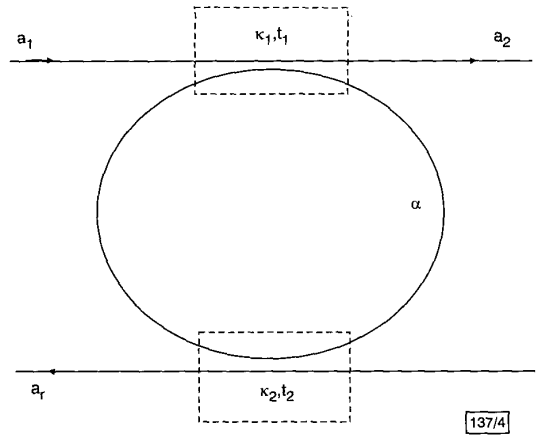

Fig. 4 *Two waveguides coupled to single ring resonator*

In summary, we have derived the generic, detail-independent, properties of circulating mode resonators coupled to one or two waveguides. We believe that these resonators will be important passive and active components of future optical circuits.

Acknowledgment: The support of the Office of Naval Research (Y.S. Park) and of the Air Force Office of Scientific Research (H. Schlossberg) is gratefully acknowledged.

16 December 1999
Electronics Letters Online No: 20000340
DOI: 10.1049/el:20000340

A. Yariv (*California Institute of Technology, Pasadena, California, USA*)

References

1 LEVI, A.F., SLUSHER, R.E., McCALL, S.L., GLASS, J.L., PEARSON, S.J., and LOGAN, R.A.: 'Directional light coupling from microdisk lasers', *Appl. Phys. Lett.*, 1993, **62**, pp. 561–563

2 KNIGHT, J.C., CHEUNG, G.F., JACQUES, F., and BIRKS, T.A.: 'Phase matched excitation of whispering gallery mode resonances by a fiber taper', *Opt. Lett.*, 1997, **22**, (15), pp. 1129

3 SLATER, J.C.: 'Microwave electronics' (D. Van Nostrand, Inc., 1950)

4 LITTLE, B.E.: 'Ultra compact Si-SiO_2 microring resonator optical channel dropping filters', *Opt. Lett.*, 1998, **23**, (20), pp. 1570

6μm vertical cavity surface emitting laser based on IV-VI semiconductor compounds

T. Schwarzl, W. Heiß, G. Springholz, M. Aigle and H. Pascher

An optically-pumped lead salt-based vertical cavity surface emitting laser is presented. The laser structure grown by molecular-beam epitaxy consists of a $Pb_{0.99}Eu_{0.01}Te$/PbTe $\lambda/2$ microcavity with $Pb_{0.99}Eu_{0.01}Te/Pb_{0.94}Eu_{0.06}Te$ Bragg mirrors. Stimulated emission was observed at 6073nm below 25K.

Coherent emitters for the mid-infrared (MIR) range are of high interest due to various gas absorption lines in this region enabling sensitive gas spectroscopy to be carried out. For these applications, usually the semiconductor lasers are made using lead salts (IV-VI) compounds [1]. Although in recent years much progress has been achieved with MIR III-V quantum cascade lasers and with type II antimony based lasers [2], lead salt lasers still have the highest CW operation temperature among electrically pumped MIR diode lasers [3]. In addition, edge emitting lead salt lasers are still the only commercially available MIR semiconductor laser sources.

In this Letter, we present an optically-pumped IV-VI vertical cavity surface emitting laser (VCSEL) with a $\lambda/2$ microcavity for a wavelength of 6μm. This represents the longest wavelength for VCSELs reported to date. In VCSELs, the planar integration of a vertical cavity directly leads to surface emission. This provides major advantages over conventional edge emitters, such as the realisation of circular beams with very low beam divergence, singlemode operation, or simplified fabrication of highly integrated high power laser arrays. However, to date, VCSELs have been fabricated only from III-V and II-VI semiconductors mainly for the near infra-red [4], but also for the MIR with the longest wavelength at 3.06μm [5].

Our IV-VI VCSEL samples consisted of two PbEuTe distributed Bragg mirrors [6] with a half wavelength PbEuTe microcavity in between. A PbTe quantum well positioned in the centre of the cavity (antinode position) was intended to be used as the active laser material. The design of the multilayer structure involved the transfer matrix method and a model for the dielectric function of the lead salts [7]. The model parameters were set for the individual materials using Fourier transform infra-red (FTIR) transmission measurements of single reference layers. Owing to the strong dependence of the energy bandgap of the lead salt compounds as compared to the microcavity resonance energy [6, 8], the VCSEL microcavity has to be tailored for a certain operation temperature. We chose 2K as the operation temperature to facilitate cooling of the optically pumped sample.

The individual $\lambda/4$ Bragg layer pairs of the mirrors consisted of $Pb_{1-x}Eu_xTe$ with alternating average Eu concentration of 1 and 6%, thus being transparent for PbTe laser emission. The thicknesses of the mirror layers for a target wavelength of 6μm at 2K were 2685 and 2935Å for $Pb_{0.99}Eu_{0.01}Te$ and $Pb_{0.94}Eu_{0.06}Te$, respectively. Fig. 1 shows a cross-sectional scanning electron microscope image of the cleavage edge of a laser sample. For bet-